Pergamon

Solid State Communications, Vol. 92, No. 5, pp. 437–442, 1994
Elsevier Science Ltd
Printed in Great Britain.
0038–1098/94 $7.00 + .00

0038–1098(94)00526–5

CALCULATION OF THE ENERGY LEVELS IN InAs/GaAs QUANTUM DOTS

J.-Y. Marzin

France Telecom, CNET-PAB, Laboratoire de Bagneux, BP107, F92225 Bagneux, France

and

G. Bastard

Laboratoire de Physique de la Matière Condensée, Ecole Normale Supérieure, 24 rue Lhomond, F75005 Paris, France

(*Received* 8 *July* 1994 *by M. Cardona*)

We present a detailed effective mass calculation of the energy levels in InAs quantum dots embedded in GaAs. We compare the results of a separable approximate treatment with a more complete numerical approach. A satisfying agreement is found with the available experimental data. Even for dot diameters of the order of 30 nm, we find large distances between consecutive energy levels, which should play an important role in the energy relaxation rates.

Keywords: A: semiconductors; A: nanostructures; D: electronic structure; D: optical properties.

1. INTRODUCTION

AFTER THE impressive development of bi-dimensional semiconductor structures and devices, numerous studies were devoted in the recent years to the fabrication and optical studies of quantum dots and wires. Among the various techniques [1] used to fabricate them, those based upon nanolithography suffer from their present limitations in terms of regularity of sizes. This partly motivates the interest in growth based techniques, where the wires or dots are more naturally formed during the growth procedure. Growth on vicinal surfaces [2–4] or non planar substrates [5–10], or on high index surfaces yielding facetting mechanisms [11] have been successfully used to fabricate quantum wire structures. As far as quantum dots are concerned, three-dimensional growth of highly mismatched material with respect to the substrate appears to be an attractive and easy means to produce quantum size dots, with a regularity of sizes still beyond the reach of most other techniques. Efficient photoluminescence (PL) of such objects were reported ten years ago for InAs/GaAs system, and numerous detailed studies [12–20] (growth, microscopy, optical properties) were devoted to this particular system. The PL emission of a single InAs quantum dot could finally be observed recently [21]. Up to now no theoretical calculation of the energy levels in these quantum structures was published to our knowledge, and this is the topic of the present paper.

InAs islands are formed naturally when an InAs layer whose thickness exceeds 1.7 monolayers (ML) [13, 18] is deposited on 1 0 0 GaAs by molecular beam epitaxy (MBE). As shown by atomic force microscopy (AFM) [20], they consist of small pyramids with a square base in the 1 0 0 plane. Their limiting planes are very close to 4 1 0 planes. They lie upon a 2D InAs layer whose thickness varies with the quantity of deposited InAs. The first step of the calculation is to approximate these pyramids by cones (height, h; base radius, r_c) having the same height (in the z growth direction) and base surface. The base angle of the cone is thus close to 12°. This very small angle allows us to assume that the strain state for InAs is the same as in a 2D layer. We assume a conduction band discontinuity equal to 95% of the difference between the GaAs band gap and the InAs band gap when this material experiences the hydrostatic component of the strain. This figure was earlier

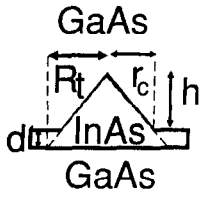

Fig. 1. Schematic cross-section of an InAs cluster.

deduced from the optical study of InAs quantum wells in GaAs [19]. It yields a type I situation for both heavy and light holes. The light-hole ($|3/2, \pm 1/2\rangle_z$) band of the strained InAs material is, however, much closer in energy of the (unstrained) GaAs valence band than the heavy hole ($|3/2, \pm 3/2\rangle_z$) band. The consequences of this band situation is twofold: (i) decoupling of the heavy and light hole problems is a good approximation; (ii) for most experimental geometries, the first light hole level is very close to GaAs valence band edge. We will calculate independently the electron, heavy and light hole levels, neglecting excitonic effects. Due to the cylindrical symmetry, these are 2D problems where unfortunately the potential is not separable and couples the motions along z (growth axis) and r (in plane radial coordinate). The one-particle Hamiltonian can be written, using the notations of Fig. 1 for the geometrical factors and taking the band edges of GaAs as energy origin

$$H_{e(h)} = E^z_{ce(h)} + E^{r,\theta}_{ce(h)} + V_{e(h)}(z,r) \tag{1}$$

with

$$E^z_{ce(h)} = -\frac{\hbar^2}{2}\left(\frac{\partial}{\partial z}\frac{1}{m^z_{e(h)}(z,r)}\frac{\partial}{\partial z}\right), \tag{2}$$

$$E^{r,\theta}_{ce(h)} = -\frac{\hbar}{2}\left(\frac{1}{r}\frac{\partial}{\partial r}\frac{r}{m^r_{e(h)}(z,r)}\frac{\partial}{\partial r} + \frac{1}{m^r_{e(h)}(z,r)}\frac{1}{r^2}\frac{\partial^2}{\partial\theta^2}\right) \tag{3}$$

and

$$\begin{aligned} V_{e(h)}(z,r) = {} & V^{\mathrm{InAs}}_{e(h)} Y(z-d)\,Y(d+h-z) \\ & \times Y[h-z-r\tan(\alpha)] \\ & + V^{\mathrm{InAs}}_{e(h)} Y(z)\,Y(d-z), \end{aligned} \tag{4}$$

where Y is the Heavyside function. $m^z_{e(h)}(z,r)$ and $m^r_{e(h)}(z,r)$ are the electron (hole) effective masses for the motion along z or in the layer planes, both depending on r and z if they are taken to be different in the two materials with

$$\begin{aligned} m^z_{e(h)}(z,r) = {} & m^{z,\mathrm{GaAs}}_{e(h)} + (m^{z,\mathrm{InAs}}_{e(h)} - m^{z,\mathrm{GaAs}}_{e(h)}) \\ & \times \{Y(z-d)\,Y(d+h-z) \\ & \times Y[h-z-r\tan(\alpha)] \\ & + Y(z)\,Y(d-z)\} \end{aligned} \tag{5}$$

and the identical expression for $m^r_{e(h)}(z,r)$.

It is clear from equations (1)–(5) that the Hamiltonian given in equation (1) is not separable in z and r. This is due to the non-separability of the potential and is still true if a constant effective mass is taken in the whole structure.

2. SEPARABLE APPROXIMATION

Let us first assume material independent effective masses in the structure so that equations (2) and (3) simply give, for the eigenstates with a $e^{in\theta}$ dependence

$$E^z_{ce(h)} = -\frac{\hbar^2}{2m^z_{e(h)}}\frac{\partial^2}{\partial z^2}$$

and (6)

$$E^r_{ce(h)} = -\frac{\hbar^2}{2m^r_{e(h)}}\left(\frac{1}{r}\frac{\partial}{\partial r}r\frac{\partial}{\partial r} - \frac{n^2}{r^2}\right).$$

Following the approach of [22–23], developed for the calculation of energy levels in quantum wires, the potential can be written

$$V_{e(h)}(z,r) = V^{QW}_{e(h)}(z) + \Delta V_{e(h)}(z,r), \tag{7}$$

where the first term of the sum is the potential of an InAs quantum well extending from $z=0$ to $z=d+h$. The lowest energy eigenstate ($n=0$) is then sought as a separable wavefunction

$$f_{e(h)}(z,r) = \phi_{e(h)}(r)\gamma_{e(h)}(z), \tag{8}$$

where $\gamma_{e(h)}(z)$ is the lowest energy eigenstate of $V^{QW}_{e(h)}$ of energy $E^1_{ze(h)}$, which varies as $A\cos(z-d/2-h)$ for $0<z<d+h$.

$\phi_{e(h)}(r)$ is then solution of

$$\begin{aligned} H^{\mathrm{eff}}_{e(h)}\phi_{e(h)}(r) = {} & [E^r_c + V^{\mathrm{eff}}_{e(h)}(r) \\ & + E^1_{ze(h)}]\phi_{e(h)}(r) = E\phi_{e(h)}(r), \end{aligned} \tag{9}$$

with $V_{\mathrm{eff}}(r) = -V^{\mathrm{InAS}}P_w(r)$ for $r < r_c$ and $V_{\mathrm{eff}}(r) = -V^{\mathrm{InAs}}P_w(r_c)$ for $r >= r_c$.

$$\begin{aligned} P_w(r) = {} & \frac{A^2}{2}h\frac{r}{r_c} \\ & \times \left\{1 + \frac{r_c\sin[kh(r/r_c)]}{khr}\cos\left[kd + kh\left(1-\frac{r}{r_c}\right)\right]\right\} \end{aligned} \tag{10}$$

is, for $r < r_c$, the probability of finding the particle of wave function $\gamma(z)$ between $z = d + h(1 - r/r_c)$ and $z = d + h$. For small r values, $V_{\text{eff}}(r)$ is linear in r and

$$V_{\text{eff}}(r) = -V^{\text{InAs}} \frac{A^2}{2} h \frac{r}{r_c} \{1 + \cos[k(d+h)]\} = eFr. \tag{10}$$

Equation (9) can be solved numerically, but one can also use the approximation of equation (10). With this form of the potential, we can have a variational estimate of E with a trial function $\phi(r) = Be^{-r/\lambda}$. The minimization of $\langle\phi|H_{\text{eff}}|\phi\rangle$ yields

$$\lambda_{e(h)} = \left(\frac{m^r_{e(h)} eF}{\hbar^2}\right)^{-1/3}$$

$$\text{and} \quad E^l_{e(h)} = E^1_{ze(h)} + \frac{3\hbar^2}{2m^r_{e(h)}} \left(\frac{m^r_{e(h)} eF}{\hbar^2}\right)^{2/3}. \tag{11}$$

As will be seen in the following, this variational calculation gives excellent results with the geometry of real InAs clusters.

3. EXACT CALCULATION

Our numerical approach to the problem is to enclose the cluster inside a cylinder of radius R and height Z_c on the surface of which the wave functions are forced to vanish. Taking into account the commutation of H and $\partial/\partial\theta$ the eigenfunctions of equation (1) satisfying these boundary conditions can be decomposed on the basis formed by products of Bessel functions of integer order n by sine functions of z

$$\chi_n(r,z,\theta) = \sum_{i>0,j>0} A^n_{i,j} \xi^n_{i,j}(z,r,\theta),$$

$$\xi^n_{i,j}(z,r,\theta) = \beta^n_i J_n(k^n_i r) e^{in\theta} \sin(K_j z), \tag{12}$$

where $k^n_i R$ is the ith zero of the Bessel function of integer order $J_n(x)$, $K_j = 2j\pi/Z_c$ and where the normalization factor β^n_i is given by

$$\beta^n_i = \sqrt{\frac{8}{v}} \frac{2}{|J_{n-1}(k^n_i R) - J_{n+1}(k^n_i R)|} \tag{13}$$

and v is the volume of the cylinder $\pi Z_c R^2$.

Each value of n yields a family of solutions. The matrix elements are given by

$$\langle\xi^n_{i,j}|E^z_{ce(h)}|\xi^n_{l,m}\rangle = \frac{\hbar^2 K_j K_m}{2} \beta^n_i \beta^n_l \int_0^R 2\pi r dr J_n(k^n_i r) J_n(k^n_l r) F_{j,m}(r), \tag{14}$$

$$F_{j,m}(r) = \int_0^{Z_c} dz \frac{\cos(K_j z)\cos(K_m z)}{m^z_{e(h)}(z,r)}, \tag{15}$$

$$\langle\xi^n_{i,j}|E^r_{ce(h)}|\xi^n_{l,m}\rangle = \frac{\hbar^2 k^n_i k^n_l}{2} \beta^n_i \beta^n_l \int_0^R 2\pi r dr [J_{n+1}(k^n_i r) J_{n+1}(k^n_l r) - J_{n-1}(k^n_i r) J_{n-1}(k^n_l r)] G_{j,m}(r), \tag{16}$$

$$G_{j,m}(r) = \int_0^{Z_c} dz \frac{\sin(K_j z)\sin(K_m z)}{m^z_{e(h)}(z,r)}, \tag{17}$$

$$\langle\xi^n_{i,j}|V_{ce(h)}|\xi^n_{l,m}\rangle = V^{\text{InAs}}_{e(h)} \times \left[O_{j,m}\delta_{il} + \beta^n_i \beta^n_l \int_0^{r_c} 2\pi r dr J_n(k^n_i r) J_n(k^n_l r) P_{j,m}(r)\right], \tag{18}$$

$$O_{j,m} = \int_0^d dz \sin(K_j z)\sin(K_m z),$$

$$P_{j,m}(r) = \int_d^{d+r\tan(\alpha)} dz \sin(K_j z)\sin(K_m z). \tag{19}$$

The form factors F, G, O and P are calculated analytically so that each matrix element involves only a one-dimensional numerical integration.

When one assumes a unique effective mass throughout the structure, the kinetic energy terms are diagonal in the $\xi^n_{i,j}$ basis and two different elements of the basis are coupled only by the potential energy terms.

In this completely numerical approach, it is easy to take into account the modifications of the potential due to the indium segregation [24] occurring when the InAs island is overgrown with GaAs. The top InAs monolayer (ML) at a given r is then slowly incorporated in the overgrowing GaAs layer, resulting in the formation of an alloy. The indium composition profile in the z growth direction can be approximated by $x(z) = (a_0/l)e^{-(z-z_0)/l}$, where a_0 is the thickness of one InAs ML. Assuming that the inverse masses and potential vary linearly with $x(z)$, this only modify the form factors F, G, O and P which are still easily integrated analytically. This effect is, however, important for the comparison with experimental optical data. We finally performed calculations

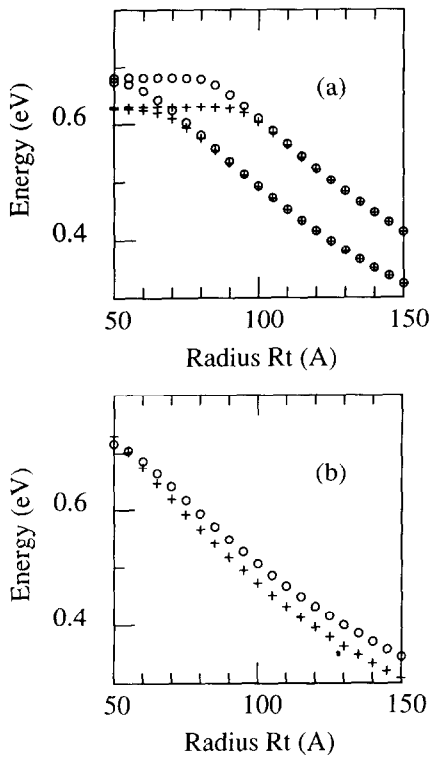

Fig. 2. (a) Confinement energies of the first two electron levels obtained in the exact calculation as a function of the cluster radius R_t, as defined in Fig. 1, for d corresponding to 1 ML (○) and 2 ML (+). (b) Confinement energy of the fundamental electron level for d corresponding to 1 ML, in the approximation of a separable wavefunction given by equation (8) (○), and evaluated by equation (11) (+), as a function of R_t.

including to some extent the difference in the electron effective masses in GaAs and InAs. We first assume for very small r_c values an electron effective mass equal to its value for GaAs conduction band edge. At any subsequent r_c, a value corresponding to the InAs conduction band effective mass in strained InAs at the energy of the electron level obtained for $r_c - dr$, if dr is the step of radius from one calculation to the next. This procedure, where non-diagonal kinetic energy terms appear through equations (15) and (17), however, yielded only slight corrections (some meV) on the transitions energies, to be compared to the tens of meV induced by the effect of indium segregation, so that this small correction is not included in the following results.

4. RESULTS AND DISCUSSION

Figure 2(a) shows the first two calculated electron levels, in this latter numerical approach, for the parameters listed in Table 1, as a function of the

Table 1. Material parameters used for the calculations

	V_{InAs} (eV)	$m_z(m_0)$	$m_r(m_0)$	E_a (InAs)
Electron	−0.697	0.067	0.067	
Heavy hole	0.288	−0.34	−0.11	0.533
Light hole	0.117	−0.09	−0.21	0.703

radius R_t of the cluster, for d corresponding to 1 and 2 ML, without inclusion of the indium segregation. For this calculation $Z_c = R = 40$ nm and the basis is formed from 25 sines and 25 Bessel functions for each value of n. Note that R_t is equal to $r_c + d\cot g(\alpha)$. No indium segregation was included in the calculation. For small R_t values, the levels saturate towards the energy of the first bound level in an InAs quantum well of thickness d (as it should). At high R_t values, where $h + d$ becomes significantly larger than d, quite similar results are obtained for the two values of d. The reason for that appears quite clearly in Fig. 3 which displays for the first electron level at $R_t = 13.5$ nm ($h = 2.6$ nm) the surface of constant $|\chi^2|$ defining a volume θ with $\int_\theta \chi^2 d\theta = 0.7$. The electron is indeed quite localized on the cone and does not feel the surrounding InAs quantum well. Another striking result shown in Fig. 2(a) is the large energy distance between the two first electron level for $R_t > 5$ nm.

Approximate results given by the numerical integration of equation (9) and by equation (11) are shown in Fig. 2(b). They correspond on most R_t range to a very good estimate of the eigenenergy. The best result is given by equation (11) and this fact is somewhat coincidental. The assumption of separability in z and r in equation (8) leads to an

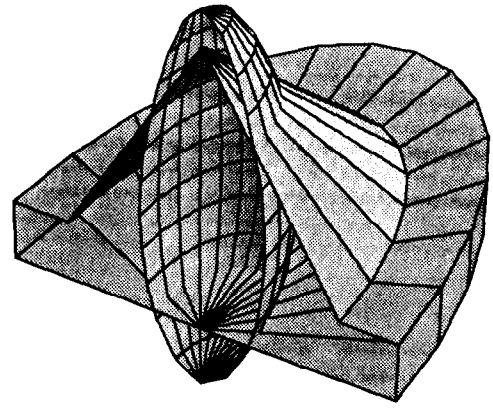

Fig. 3. Isovalue surface of the first electron squared eigenfunction for $R_t = 13.5$ nm and d corresponding to 2 ML, enclosing the volume in which the integrated probability of finding the electron is 0.7. The potential profile is also indicated in the figure, which is dilated in the z growth direction.

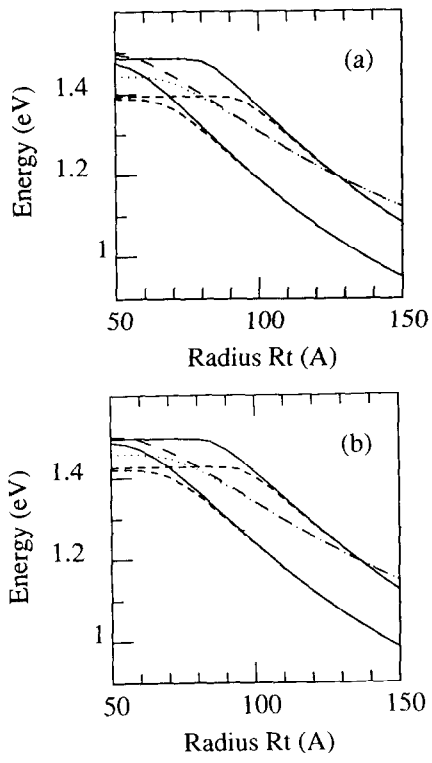

Fig. 4. First two heavy-hole and first light-hole allowed transition energies as a function of R_t without (a), and with (b) inclusion of the effect of indium segregation ($l = 1.1$ nm). d correspond to 1 ML (- - - -; heavy hole, - - -; light hole) θ or 2 ML (- - -, heavy hole; · · · · ·, light hole).

overestimate of the eigenenergy [as seen when comparing Fig. 2(a) and (b)], and the variational form of the radial function for equation (11) does so too. These effects are compensated by the underestimate of the effective potential $V^{\text{eff}}_{e(h)}(r)$ given by equation (10).

Figure 4(a) displays the calculated energies for the two first heavy and first light-hole allowed transitions between electron and heavy hole states. The calculation was done for d corresponding to 1 or 2 InAs ML, again without indium segregation. The transitions tend at low R_t values towards the continuum transitions associated to this underlying InAs quantum well. In Fig. 4(b), the effect of indium segregation was included ($l = 1.1$ nm), and, for a given R_t, the energies of the transitions increase with respect to the previous case.

For this latter case, an excellent agreement is obtained with available experimental data. For the same InAs overall content, AFM (in a sample without GaAs overgrowth) and photoluminescence data (in a sample with GaAs overgrowth) allowed us to determine both the geometry and low temperature emission energy [19]. The average radius would correspond in these samples to $R_t = 13.5$ nm which emit at 1.07 eV at 10 K. Special care was taken to interrupt the growth in the overgrown sample between InAs and subsequent GaAs deposition. This is essential because the InAs islands evolve during such an interrupt and reach equilibrium only after 10 to 15 s [19]. The AFM measurements are done on islands that have indeed evolved towards this quasi-equilibrium. This good agreement, together with the large distance between the first two allowed transitions strongly indicate that the PL emission corresponds to the fundamental transition. This calculation can thus in turn be used to estimate the sizes of InAs clusters buried in GaAs, and this was done in [21].

Our calculations show that the energy distance between the fundamental and first excited electron and hole states are significantly larger than the longitudinal optical phonon energy for actual R_t values. In this situation, several theoretical works [25–29] conclude that the carrier capture inside the dots should be very slow, as compared to typical recombination times inside the barrier material or to realistic non-radiative recombination times. The experimentally observed high energy relaxation rates in these structures are thus still to be explained. Dots with R_t smaller than 8 nm would be ideal objects to study the capture of carriers photocreated in the continuum levels toward a single electron and hole bound states. For R_t larger than about 8 nm (respectively 10 nm), there is at least one excited transition between the lowest (resp first excited) electron and lowest light hole (respectively first excited heavy hole) levels which should allow to excite resonantly the quantum dot and study in more detail the relaxation between these states. Finally, if the simple approach we have presented here is a good starting point for analysing experimental data, excitonic effects play an important role in these structures [29] and have to be taken into account in a further step.

Acknowledgement – The authors are grateful to J.M. Gerard for his fruitful comments. Part of this work was funded through EEC ESPRIT Basic Research Actions NANOPT and GOODS. Our laboratories are "unités associées au CNRS" (UA1437 and UA250 respectively).

REFERENCES

1. K. Kash, *J. Luminesc.* **46,** 69 (1990) (and references therein).
2. P.M. Petroff, A.C. Gossard & W. Wiegmann, *Appl. Phys. Lett.* **45,** 620 (1984).

3. M.S. Miller, C.E. Prior, H. Weman, L.A. Samoska, H. Kroemer & P.M. Petroff, *J. Cryst. Growth* **111,** 323 (1991).
4. M. Tanaka & H. Sakaki, *Appl. Phys. Lett.* **54,** 1326 (1989).
5. E. Colas, E. Kapon, S. Simhony, H.M. Cox, R. Bhat, K. Kash & P.S. Lin, *Appl. Phys. Lett.* **55,** 867 (1989).
6. E. Kapon, J.P. Harbison, C.P.Yun & N.G. Stoffel, *Appl. Phys. Lett.* **52,** 607 (1988).
7. E. Kapon, D.W. Hwang, M. Walther, R. Bhat & N.G. Stoffel, *Surf. Sci.* **267,** 593 (1992).
8. S. Tsukamoto, Y. Nagamune, M. Nishioka & Y. Arakawa, *J. Appl. Phys.* **71,** 533 (1992).
9. H. Asai, S. Yamada & T. Fukui, *Appl. Phys. Lett.* **51,** 1518 (1987).
10. Y. Nakamune, S. Tsukamoto, M. Nishioka & Y. Arakawa, *Proc. Int. Conf. Solid States Devices and Materials 1991.* Yokohama, Japan (1991).
11. R. Notzel, N.N. Ledentsov, L. Daweritz & K. Ploog, *Phys. Rv.* **B45,** 3507 (1992).
12. W.J. Schaffer, M.D. Lind, S.P. Kowalczyk & R.W. Grant, *J. Vac. Sci. Technol.* **B1,** 688 (1983).
13. L. Goldstein, F. Glas, J.Y. Marzin, M.N. Charasse & G. Le Roux, *Appl. Phys. Lett.* **47,** 1099 (1985).
14. H. Ohno, R. Katsumi, T. Takama & H. Hasegawa, *Jpn. J. Appl. Phys.* **24,** L682 (1985).
15. F.J. Grunthaner, M.Y. Yen, R. Fernandez, T.C. Lee, A. Madhukar & B.F. Lewis, *Appl. Phys. Lett.* **46,** 983 (1985).
16. C. Houzay, C. Guille, J.M. Moison, P. Henoc & F. Barthe, *J. Cryst. Growth* **81,** 67 (1987).
17. F. Glas, C. Guille, P. Henoc & F. Houzay, *Int. Phys. Conf. Ser.* **87,** 71 (1987).
18. J.M. Gérard, *Appl. Phys. Lett.* **61,** 2096 (1992).
19. J.M. Gérard, in *Confined Electrons and Photons: New Physics and Applications,* (Edited by C. Weisbuch & E. Burstein), to be published by Plenum.
20. J.M. Moison, F. Houzay, F. Barthe, L. Leprince, E. André & O. Vatel, *Appl. Phys. Lett.* **64,** 196 (1994).
21. J.-Y. Marzin, J.-M. Gérard, A. Izraël, D. Barrier & G. Bastard, *Phys. Rev. Lett.* **73,** 716 (1994).
22. Y.C. Chang, L.L. Chang & L. Esaki, *Appl. Phys. Lett.* **47,** 1324 (1985).
23. G. Bastard, J.A. Brum & R. Ferreira, *Solid State Phys.* **44,** (Edited by H. Ehrenreich & D. Turnbull) p.229, Academic Press, New York (1991).
24. J.M. Moison, C. Guille, F. Houzay, F. Barthe & M. Van Rompay, *Phys. Rev.* **B40,** 6149 (1989).
25. U. Bockelmann & G. Bastard, *Phys. Rev.* **B42,** 8947 (1990).
26. H. Benisty, C.M. Sottomayor-Torres & C. Weisbuch, *Phys. Rev.* **B44,** 10945 (1991).
27. T. Inoshita & H. Sakaki, *Phys. Rev.* **B46,** 7260 (1992).
28. U. Bockelmann & T. Egeler, *Phys. Rev.* **B46,** 15574 (1992).
29. U. Bockelmann, *Phys. Rev.* **B48,** 17637 (1993).